Observability and Estimability of Collaborative Opportunistic Navigation with Pseudorange Measurements

Zaher M. Kassas and Todd E. Humphreys
The University of Texas at Austin

BIOGRAPHIES

Zaher M. Kassas is pursuing a Ph.D. in the Department of Electrical and Computer Engineering at The University of Texas at Austin. He received a B.E. in Electrical Engineering with Honors from The Lebanese American University, M.S. in Electrical and Computer Engineering from The Ohio State University, and M.S.E. in Aerospace Engineering from The University of Texas at Austin. He is a member of the UT Radionavigation Laboratory. His research interests include estimation and filtering, control systems, intelligent autonomous systems (UAVs and UGVs), and navigation.

Todd E. Humphreys is an assistant professor in the department of Aerospace Engineering and Engineering Mechanics at the University of Texas at Austin, and Director of the UT Radionavigation Laboratory. He received a B.S. and M.S. in Electrical and Computer Engineering from Utah State University and a Ph.D. in Aerospace Engineering from Cornell University. He specializes in applying optimal estimation and signal processing techniques to problems in radionavigation. His recent focus is on radionavigation robustness and security.

ABSTRACT

The observability and estimability of collaborative opportunistic navigation (COpNav) environments are studied. A COpNav environment can be thought of as a radio frequency signal landscape within which one or more radio frequency receiver locate themselves in space and time by extracting and possibly sharing information from ambient signals of opportunity (SOPs). Available SOPs may have a fully-known, partially-known, or unknown characterization. In the present work, the receivers are assumed to draw only pseudorange-type measurements from the SOPs. Separate observations are fused to produce an estimate of each receiver's position, velocity, and time (PVT). Since not all SOP states in the COpNav environment may be known *a priori*, the receivers must estimate the unknown SOP states of interest simultaneously with their own PVT. This paper establishes the minimal conditions under which a COpNav environment consisting of multiple receivers and multiple SOPs is completely observable. In scenarios where the COpNav environment is not completely observable, the observable states, if any, are specified. Moreover, for the completely observable scenarios, the degree of observability, commonly referred to as estimability, of the various states is studied, with particular attention paid to the states with exceptionally good and poor observability.

I. INTRODUCTION

Opportunistic navigation (OpNav) aims to extract positioning and timing information from ambient radio-frequency "signals of opportunity" (SOPs). OpNav radio receivers continuously search for opportune signals from which to draw navigation and timing information, employing on-the-fly signal characterization as necessary. Signals from discovered SOPs are downmixed and sampled coherently, yielding a tight coupling between signal streams that permits carrier-phase-level fusion of observables from the various streams within a single or distributed state estimator [1, 2].

The Global Positioning System (GPS) control segment routinely solves an instance of the OpNav problem: the location and timing offsets of a dozen or more GPS ground stations are simultaneously estimated together with the orbital and clock parameters of the GPS satellites [3]. Compared to the general OpNav problem, the GPS control segment's problem enjoys the constraints imposed by accurate prior estimates of site locations and satellite orbits. Moreover, estimation of clock states is aided by the presence of highly-stable atomic clocks in the satellites and at each ground station. In contrast, an OpNav receiver entering a new signal landscape may have less prior information to exploit and typically cannot assume atomic frequency references, either for itself or for the SOPs. The GPS control segment example also highlights the essentially collaborative nature of OpNav. Like the GPS ground stations, multiple OpNav receivers can share information to construct and continuously-refine a global signal landscape. The multi-receiver generalization of OpNav is termed cooperative opportunistic navigation (COpNav). The large size of the COpNav estimation problem, naturally raises the question of state observability.

**Preprint of the 2012 ION GNSS Conference
Nashville, TN, September 17–21, 2012**

In its most general form, OpNav treats all ambient radio signals as potential SOPs, from conventional global navigation satellite system (GNSS) signals to communications signals never intended for use as a timing or positioning source. Each signal's relative timing and frequency offsets, transmit location, and frequency stability, are estimated on-the-fly as necessary, with prior information about these quantities exploited when available. At this level of generality, the OpNav estimation problem is similar to the so-called simultaneous localization and mapping (SLAM) problem in robotics [4]. Both imagine an actor which, starting with incomplete knowledge of its location and surroundings, simultaneously builds a map of its environment and locates itself within that map.

In traditional SLAM, the map that gets constructed as the actor (typically a robot) moves through the environment is composed of landmarks—walls, corners, posts, etc.—with associated positions. OpNav extends this concept to radio signals, with SOPs playing the role of landmarks. In contrast to a SLAM environmental map, the OpNav "signal landscape" is dynamic and more complex. For the simple case of pseudorange-only OpNav, where observables consist solely of signal time-of-arrival measurements, one must estimate, besides the three-dimensional position $\boldsymbol{x}_s$ and velocity $\dot{\boldsymbol{x}}_s$ of each SOP transmitter's antenna, each SOP's time offset δt_s from a reference time base, rate of change of time offset $\dot{\delta t}_s$, and a small set of parameters that characterize the SOP's reference oscillator stability. Even more SOP parameters are required for an OpNav framework in which both pseudorange and carrier phase measurements are ingested into the estimator [1]. Of course, in addition to the SOP parameters, the OpNav receiver's own three-dimensional position $\boldsymbol{x}_r$ and velocity $\dot{\boldsymbol{x}}_r$, time offset δt_r, and time offset rate $\dot{\delta t}_r$ must be estimated.

A study of COpNav observability benefits from the COpNav-SLAM analogy. Although the question of observability was not addressed for more than a decade after SLAM was introduced, the recent SLAM literature has come around to considering fundamental properties of the SLAM problem, including observability [5–9]. The effects of partial observability in planar SLAM with range and bearing measurements were first analyzed via linearization by Andrade-Cetto and Sanfeliu [5]. This paper came to the counterintuitive conclusion that the two-dimensional planar wold-centric (absolute reference frame) SLAM problem is fully-observable when the location of a single landmark is known *a priori*. With a fully nonlinear observability analysis, Lee et al. subsequently disproved this result and showed that at least two anchor landmarks with known positions are required for local weak observability [7]. Later analysis of the SLAM problem's Fisher information matrix confirmed the result of the nonlinear analysis [8]. However, an apparent discrepancy between linear and nonlinear SLAM observability analyses re-emerged in the work of Perera and Nettleton [9], where it was shown that a linear analysis based on piecewise constant system (PWCS) theory [10] again predicted global planar-SLAM observability in the case of a single known anchor landmark, whereas a nonlinear analysis in the same paper indicated that two known anchor landmarks were required for local observability. The linear PWCS result appears flawed given that an observability test based on linearization should never predict observability in a case where a fully nonlinear test indicates lack of local weak observability.

An initial OpNav observability analysis was conducted in [11]. It considered several scenarios which could be encountered in a typical OpNav environment comprising a single receiver and multiple stationary SOPs. The OpNav observability analysis in [11] utilized nonlinear local weak observability tests, linear time-varying (LTV) observability tests, and PWCS observability tests. While the conclusions achieved by the former two methods agreed, the PWCS observability tests yielded contradictory results, similar to the ones encountered in the SLAM observability analysis. As clarified in [11], a close examination of PWCS observability theory reveals that it is inapplicable to systems whose measurement model is nonlinear.

The present paper's contribution is to extend the work of [11] in two ways. First, it considers the case of a COpNav environment, which comprises multiple receivers in an environment with multiple SOPs. The receivers are assumed to share information about the environment. Subsequently, the minimum set of information necessary to make the COpNav environment completely observable is established. The second contribution is to analyze the estimability of the COpNav environment. Whereas the notion of observability is a binary property, i.e. it specifies whether the system is observable or not; for estimation purposes, the question of stochastic observability, also referred to as estimability, is of considerable importance. Estimability assesses the "degree of observability" of the various states. Not only is estimability vital for assessing the performance of the estimators in a COpNav environment, but it also could aid in prescribing maneuvers necessary to maintain accurate estimates of the receiver and signal landscape map. The observability and estimability results offered are verified through simulations.

The remainder of this paper is organized as follows. Section II reviews the various notions and tools necessary to analyze the observability and estimability of COpNav environments. Section III describes the COpNav environment dynamics and observation model considered in this paper. Section IV analyzes various COpNav scenarios and establishes whether each scenario is observable. This leads to a set of minimum conditions necessary for complete COpNav observability. Section V analyzes the estimability of the COpNav states through simulating various COpNav scenarios. Concluding remarks are given in Section VI.

II. THEORETICAL BACKGROUND

Conceptually, observability of a dynamic system boils down to the question of solvability of the state from a set of observations that are linearly or nonlinearly related to the state, and where the state evolves according to a set of linear or nonlinear difference or differential equations. In particular, observability is concerned with determining whether the state of the system can be consistently estimated from a set of observations taken over a finite period of time.

For nonlinear systems, it is more appropriate to analyze the observability through nonlinear observability tools rather than linearizing the nonlinear system and applying linear observability tools. This is due to two reasons: (i) nonlinear observability tools capture the nonlinearities of the dynamics and observations, and (ii) while the control inputs are never considered in the linear observability analysis, they are taken into account in the nonlinear observability analysis.

A. Observability of Nonlinear Systems

For the sake of clarity, various notions of nonlinear observability are defined in this subsection [12].

Definition 1. *Consider the continuous-time (CT) nonlinear dynamic system*

$$\Sigma_{\text{NL}}: \begin{cases} \dot{\boldsymbol{x}}(t) = \boldsymbol{f}\left[\boldsymbol{x}(t), \boldsymbol{u}(t)\right], & \boldsymbol{x}(t_0) = \boldsymbol{x}_0 \\ \boldsymbol{y}(t) = \boldsymbol{h}\left[\boldsymbol{x}(t)\right], \end{cases} \tag{1}$$

with solution $\boldsymbol{x}(t) = \boldsymbol{g}\left(t, \boldsymbol{x}_0, \boldsymbol{u}\right)$, where $\boldsymbol{x} \in \mathbb{R}^n$ is the system state vector, $\boldsymbol{u} \in \mathbb{R}^r$ is the control input vector, $\boldsymbol{y} \in \mathbb{R}^m$ is the observation vector, and $\boldsymbol{x}_0$ is an arbitrary initial condition. Two states $\boldsymbol{x}_1$ and $\boldsymbol{x}_2$ are said to be indistinguishable if $\boldsymbol{h}[\boldsymbol{g}\left(t, \boldsymbol{x}_1, \boldsymbol{u}\right)] = \boldsymbol{h}[\boldsymbol{g}\left(t, \boldsymbol{x}_2, \boldsymbol{u}\right)]$, for all $t \geq 0$ and all $\boldsymbol{u}$. The set of all points indistinguishable from a particular state $\boldsymbol{x}$ is denoted as $\mathbb{I}(\boldsymbol{x})$.

Definition 2. *Let $\mathfrak{N}$ be a subset (neighborhood) in the state-space $\mathbb{R}^n$ and $\boldsymbol{x}_1, \boldsymbol{x}_2 \in \mathfrak{N}$. Two states $\boldsymbol{x}_1$ and $\boldsymbol{x}_2$ are said to be $\mathfrak{N}$-indistinguishable if every control $\boldsymbol{u}$, whose trajectories from $\boldsymbol{x}_1$ and $\boldsymbol{x}_2$ both lie in $\mathfrak{N}$, fails to distinguish between $\boldsymbol{x}_1$ and $\boldsymbol{x}_2$. The set of all $\mathfrak{N}$-indistinguishable states from a particular state $\boldsymbol{x}$ is denoted as $\mathbb{I}_{\mathfrak{N}}(\boldsymbol{x})$.*

Definition 3. *The system Σ_{NL} is said to be observable at $\boldsymbol{x}_0$ if $\mathbb{I}(\boldsymbol{x}_0) = \{\boldsymbol{x}_0\}$. The system Σ_{NL} is said to be observable if $\mathbb{I}(\boldsymbol{x}_0) = \{\boldsymbol{x}_0\}$, for all $\boldsymbol{x}_0 \in \mathbb{R}^n$.*

Note that observability is a global concept. It might be necessary to travel a considerable distance or for a long period of time to distinguish between initial conditions in $\mathbb{R}^n$. Moreover, observability of Σ_{NL} does not imply that every input $\boldsymbol{u}$ distinguishes initial conditions in $\mathbb{R}^n$.

Definition 4. *The system Σ_{NL} is said to be locally observable at $\boldsymbol{x}_0$ if $\mathbb{I}_{\mathfrak{N}}(\boldsymbol{x}_0) = \{\boldsymbol{x}_0\}$ for every open neighborhood $\mathfrak{N}$ of $\boldsymbol{x}_0$.*

Note that local observability is stronger than observability. Local observability requires distinguishability of the initial conditions without going too far. In particular, trajectories need to lie in *any* open subset of $\mathbb{R}^n$.

Definition 5. *The system Σ_{NL} is said to be weakly observable at $\boldsymbol{x}_0$ if there exists a neighborhood $\mathfrak{N}$ such that $\mathbb{I}(\boldsymbol{x}_0) \bigcap \mathfrak{N} = \{\boldsymbol{x}_0\}$.*

Note that weak observability is weaker than observability. Weak observability requires the existence of an open subset in $\mathbb{R}^n$ within which the only initial condition that is indistinguishable from $\boldsymbol{x}_0$ is $\boldsymbol{x}_0$ itself. Note that in weakly observable systems, trajectories may need to travel far enough for distinguishability of the initial conditions.

Definition 6. *The system Σ_{NL} is said to be locally weakly observable at $\boldsymbol{x}_0$ if there exists an open neighborhood $\mathfrak{N}$ of $\boldsymbol{x}_0$ such that for every open neighborhood $\mathfrak{M}$ of $\boldsymbol{x}_0$ with $\mathfrak{M} \subset \mathfrak{N}$, $\mathbb{I}_{\mathfrak{M}}(\boldsymbol{x}_0) = \{\boldsymbol{x}_0\}$.*

Intuitively, Σ_{NL} is locally weakly observable if $\boldsymbol{x}$ can be instantaneously distinguished from its neighbors. The various notions of observability are related to each other according to the following relationships

$$\begin{array}{ccc} \text{locally observable} & \Rightarrow & \text{observable} \\ \Downarrow & & \Downarrow \\ \text{locally weakly observable} & \Rightarrow & \text{weakly observable.} \end{array}$$

For nonlinear systems, establishing global system properties, such as observability, is typically difficult to achieve. Hence, local properties are typically sought. A somewhat simple algebraic test exists for establishing local weak observability of a specific form of the nonlinear system Σ_{NL} in (1), known as the control affine form [13], given by

$$\Sigma_{\text{NL,a}}: \begin{cases} \dot{\boldsymbol{x}}(t) = \boldsymbol{f}_0\left[\boldsymbol{x}(t)\right] + \sum_{i=1}^{r} \boldsymbol{f}_i\left[\boldsymbol{x}(t)\right] u_i, & \boldsymbol{x}(t_0) = \boldsymbol{x}_0 \\ \boldsymbol{y}(t) = \boldsymbol{h}\left[\boldsymbol{x}(t)\right]. \end{cases} \tag{2}$$

This test is based on the concept of Lie derivatives, which are defined next.

Definition 7. *The first-order Lie derivative of a scalar function h with respect to a vector-valued function $\boldsymbol{f}$ is defined as*

$$\mathfrak{L}^1_{\boldsymbol{f}} h(\boldsymbol{x}) \triangleq \sum_{j=1}^{n} \frac{\partial h(\boldsymbol{x})}{\partial x_j} f_j(\boldsymbol{x}) \tag{3}$$

$$= \left\langle \nabla_{\boldsymbol{x}} h(\boldsymbol{x}), \boldsymbol{f}(\boldsymbol{x}) \right\rangle, \tag{4}$$

where $\boldsymbol{f}(\boldsymbol{x}) \triangleq [f_1(\boldsymbol{x}), \ldots, f_n(\boldsymbol{x})]^{\mathsf{T}}$. *The zeroth-order Lie derivative of any function is the function itself, i.e.* $\mathfrak{L}^0_{\boldsymbol{f}} h(\boldsymbol{x}) = h(\boldsymbol{x})$. *The second-order Lie derivative can be computed recursively as*

$$\mathfrak{L}^2_{\boldsymbol{f}} h(\boldsymbol{x}) = \mathfrak{L}_{\boldsymbol{f}} \left[\mathfrak{L}^1_{\boldsymbol{f}} h(\boldsymbol{x})\right] \quad (5)$$

$$= \left\langle \left[\nabla_{\boldsymbol{x}} \mathfrak{L}^1_{\boldsymbol{f}} h(\boldsymbol{x})\right], \boldsymbol{f}(\boldsymbol{x}) \right\rangle. \quad (6)$$

Higher-order Lie derivatives can be computed similarly. Mixed-order Lie derivatives of $h(\boldsymbol{x})$ *with respect to different functions* $\boldsymbol{f}_i$ *and* $\boldsymbol{f}_j$, *given the derivative with respect to* $\boldsymbol{f}_i$, *can be defined as*

$$\mathfrak{L}^2_{\boldsymbol{f}_i \boldsymbol{f}_j} h(\boldsymbol{x}) \triangleq \mathfrak{L}^1_{\boldsymbol{f}_j} \left[\mathfrak{L}^1_{\boldsymbol{f}_i} h(\boldsymbol{x})\right] \quad (7)$$

$$= \left\langle \left[\mathfrak{L}^1_{\boldsymbol{f}_i} h(\boldsymbol{x})\right], \boldsymbol{f}_j(\boldsymbol{x}) \right\rangle. \quad (8)$$

Definition 8. *Given the nonlinear system in control affine form* $\Sigma_{\mathrm{NL,a}}$, *the so-called nonlinear observability matrix is defined as the matrix whose rows are the gradients of Lie derivatives, specifically*

$$\boldsymbol{\mathcal{O}}_{\mathrm{NL}} \triangleq \left\{ \nabla_{\boldsymbol{x}} \mathfrak{L}^l_{\boldsymbol{f}_i, \ldots, \boldsymbol{f}_j} h_p(\boldsymbol{x}) \,|\, i, j = 0, \ldots, l;\ l = 0, \ldots, n-1,\ p = 1, \ldots, m \right\} \quad (9)$$

Note that for the case of vector observations $\boldsymbol{h}$, we need to calculate $n-1$ derivatives for each scalar component h_p. Note also that it is enough to consider the first $n-1$ Lie derivatives of the $\boldsymbol{h}$ for the rank test and we can stop taking further derivatives of $\boldsymbol{h}$ at the first instance of linear dependence among their gradients [13].

The significance of the nonlinear observability matrix is that it can be employed to furnish necessary and sufficient conditions for local weak observability [12]. In particular, if $\boldsymbol{\mathcal{O}}_{\mathrm{NL}}$ is full-rank, then the system $\Sigma_{\mathrm{NL,a}}$ is said to satisfy the observability rank condition.

Theorem 1. *If the nonlinear system in control affine form* $\Sigma_{\mathrm{NL,a}}$ *satisfies the observability rank condition, then the system is locally weakly observable.*

Theorem 2. *If a system* $\Sigma_{\mathrm{NL,a}}$ *is locally weakly observable, then the observability rank condition is satisfied generically.*

The term "generically" means that the observability matrix is full-rank everywhere, except possibly within a subset of the domain of $\boldsymbol{x}$ [14]. Therefore, if the $\boldsymbol{\mathcal{O}}_{\mathrm{NL}}$ is not of sufficient rank for all values of $\boldsymbol{x}$, the system is not locally weakly observable [15].

B. Observability of Linear Systems

Observability of discrete-time (DT) LTV systems is defined as follows [16].

Definition 9. *Consider the DT LTV dynamic system*

$$\Sigma_{\mathrm{L}}: \begin{cases} \boldsymbol{x}(t_{k+1}) = \mathbf{F}(t_k)\boldsymbol{x}(t_k) + \mathbf{B}(t_k)\boldsymbol{u}(t_k), & \boldsymbol{x}(t_{k_0}) = \boldsymbol{x}_0 \\ \boldsymbol{y}(t_k) = \mathbf{H}(t_k)\boldsymbol{x}(t_k), & t_k \in [t_{k_0}, t_{k_f}], \end{cases} \quad (10)$$

where $\mathbf{F} \in \mathbb{R}^{n\times n}$, $\mathbf{B} \in \mathbb{R}^{n\times r}$, *and* $\mathbf{H} \in \mathbb{R}^{m\times n}$. *The LTV system* Σ_{L} *is said to be observable in a time interval* $[t_{k_0}, t_{k_f}]$, *if the initial state* $\boldsymbol{x}_0$ *is uniquely determined by the zero-input response* $\boldsymbol{y}(t_k)$ *for* $t_k \in [t_{k_0}, t_{k_f - 1}]$. *If this property holds regardless of the initial time* t_{k_0} *or the initial state* $\boldsymbol{x}_0$, *the system is said to be completely observable.*

For linear systems, if any input distinguishes the initial conditions $\boldsymbol{x}_0$, then every input does. Hence, it suffices to consider the case $\boldsymbol{u} \equiv 0$, and this is why control inputs are never considered when assessing observability of linear systems.

Observability of LTV systems Σ_{L} is typically established through studying the rank of either the so-called observability Grammian or the observability matrix. The following theorem states a necessary and sufficient condition for observability of LTV systems through the l-step observability matrix [16].

Theorem 3. *The LTV system* Σ_{L} *is* l*-step observable if and only if the* l*-step observability matrix, defined as*

$$\boldsymbol{\mathcal{O}}_L(t_k, t_{k+l}) \triangleq \begin{bmatrix} \mathbf{H}(t_k) \\ \mathbf{H}(t_{k+1})\boldsymbol{\Phi}(t_{k+1}, t_k) \\ \vdots \\ \mathbf{H}(t_{k+l-1})\boldsymbol{\Phi}(t_{k+l-1}, t_k) \end{bmatrix} \quad (11)$$

is full-rank, i.e. $\mathrm{rank}\left[\boldsymbol{\mathcal{O}}_{\mathrm{L}}(\mathrm{t_k}, \mathrm{t_{k+l}})\right] = \mathrm{n}$. *The matrix* $\boldsymbol{\Phi}$ *is the DT transition matrix, defined as*

$$\boldsymbol{\Phi}(t_k, t_j) \triangleq \begin{cases} \mathbf{F}(t_{k-1})\mathbf{F}(t_{k-2})\cdots\mathbf{F}(t_j), & t_k \geq t_{j+1}; \\ \mathbf{I}, & t_k = t_j. \end{cases}$$

Linear observability tools may be applied to nonlinear systems by expressing the nonlinear system in its linearized error form (also known as the indirect form), where the state vector $\Delta\boldsymbol{x}$ in this formulation contains the error states, which are defined as the difference between the true states and the nominal states, and the observation vector $\Delta\boldsymbol{y}$ is defined as the difference between the true observations and the nominal observations. The linearized error form of the discretized version of the nonlinear system Σ_{NL} defined in (1) is given by

$$\begin{aligned} \Delta\boldsymbol{x}(t_{k+1}) &= \mathbf{F}(t_k)\,\Delta\boldsymbol{x}(t_k) \\ \Delta\boldsymbol{y}(t_k) &= \mathbf{H}(t_k)\Delta\boldsymbol{x}(t_k), \end{aligned} \quad (12)$$

where $\mathbf{F}$ and $\mathbf{H}$ are the dynamics and observation Jacobian matrices, respectively, evaluated at the nominal states. The observability results achieved in this case are local.

C. Degree of Observability: Estimability

Whereas the notion of observability is a binary property, i.e. it specifies whether the system is observable or not; for estimation purposes, the question of estimability, is of considerable importance. Estimability assesses the "degree of observability" of the various states. Estimability can be assessed by the condition number of the FIM, thus measuring whether an observable system is poorly estimable due to the gradient vectors comprising the FIM being nearly collinear [17].

An alternative method for assessing estimability of the different states was proposed in [18]. This method is based on analyzing the eigenvalues and eigenvectors of a normalized estimation error covariance matrix of the Kalman Filter (KF). The normalization of the estimation error covariance serves two purposes. First, it forces the transformed estimation error vector to be dimensionless. This dimensional homogeneity makes comparison among the eigenvalues meaningful. Such transformation can be accomplished through the congruent transformation

$$\mathbf{P}^{'}(t_k|t_k) = \left[\sqrt{\mathbf{P}(t_0|t_{-1})}\right]^{-1} \mathbf{P}(t_k|t_k) \left[\sqrt{\mathbf{P}(t_0|t_{-1})}\right]^{-1},$$

where $\mathbf{P}(t_0|t_{-1})$ is the initial estimation error covariance and $\mathbf{P}(t_k|t_k)$ is the posterior estimation error covariance. Second, it sets a bound for the eigenvalues such that they are bounded between zero and n. This can be accomplished through

$$\mathbf{P}^{''}(t_k|t_k) = \frac{n}{\mathrm{tr}\left[\mathbf{P}^{'}(\mathrm{t_k}|\mathrm{t_k})\right]} \mathbf{P}^{'}(t_k|t_k), \tag{13}$$

where tr(•) is the trace of the matrix.

The largest eigenvalue of $\mathbf{P}^{''}(t_k|t_k)$ corresponds to the variance of the state or linear combination of states that is poorly observable. On the other hand, the state or linear combination of states that is most observable is indicated by the smallest eigenvalue. The appropriate linear combination of states yielding the calculated degree of observability is given by the respective eigenvectors. Of course, there are cases where the eigenvalues distribution is uninteresting and nothing startling is revealed by this method. However, wide dispersion of the eigenvalues indicate cases of exceptionally good or poor observability of certain linear combinations of the states [18].

III. MODEL DESCRIPTION

A. Dynamics Model

The receiver's dynamics will be assumed to evolve according to the continuous white noise acceleration model, which is also known as the velocity random walk model. An object moving according to such dynamics in a generic coordinate ξ, has the dynamics

$$\ddot{\xi}(t) = \tilde{w}_\xi(t),$$

where $\tilde{w}_\xi(t)$ is a zero-mean white noise process with power spectral density $\tilde{q}_\xi$, i.e.

$$\mathbb{E}\left[\tilde{w}_\xi(t)\right] = 0, \quad \mathbb{E}\left[\tilde{w}_\xi(t)\tilde{w}_\xi(\tau)\right] = \tilde{q}_\xi\, \delta(t-\tau),$$

where $\delta(t)$ is the Dirac delta function. The receiver and SOP clock error dynamics will be modeled according to the so-called two-state model, composed of the clock bias δt and clock drift $\dot{\delta t}$. The clock error states evolve according to

$$\dot{\boldsymbol{x}}_{\mathrm{clk}}(t) = \mathbf{A}_{\mathrm{clk}}\, \boldsymbol{x}_{\mathrm{clk}}(t) + \tilde{\boldsymbol{w}}_{\mathrm{clk}}(t),$$

where

$$\boldsymbol{x}_{\mathrm{clk}} = \begin{bmatrix} \delta t \\ \dot{\delta t} \end{bmatrix}, \quad \tilde{\boldsymbol{w}}_{\mathrm{clk}} = \begin{bmatrix} \tilde{w}_{\delta t} \\ \tilde{w}_{\dot{\delta t}} \end{bmatrix}, \quad \mathbf{A}_{\mathrm{clk}} = \begin{bmatrix} 0 & 1 \\ 0 & 0 \end{bmatrix},$$

where $\tilde{w}_{\delta t}$ and $\tilde{w}_{\dot{\delta t}}$ are zero-mean, mutually independent white noise processes with power spectra $S_{\delta t}$ and $S_{\dot{\delta t}}$, respectively. The power spectra $S_{\delta t}$ and $S_{\dot{\delta t}}$ can be related to the power-law coefficients, $\{h_\alpha\}_{\alpha=-2}^{2}$, which typically characterize the power spectral density of the fractional frequency deviation $y(t)$ of an oscillator from nominal frequency. It is common to approximate such relationships by considering only the frequency random walk coefficient h_{-2} and the white frequency coefficient h_0, which lead to $S_{\delta t} \approx \frac{h_0}{2}$ and $S_{\dot{\delta t}} \approx 2\pi^2 h_{-2}$ [17].

The receiver's state vector will be defined by augmenting the receiver's planar position and velocity states with its clock error states to yield the state-space realization

$$\dot{\boldsymbol{x}}_r(t) = \mathbf{A}_r\, \boldsymbol{x}_r(t) + \mathbf{D}_{\mathbf{r}}\, \tilde{\boldsymbol{w}}_r(t), \tag{14}$$

where $\boldsymbol{x}_r = \left[\boldsymbol{r}_r^{\mathsf{T}},\, \dot{\boldsymbol{r}}_r^{\mathsf{T}},\, \delta t_r,\, \dot{\delta t}_r\right]^{\mathsf{T}}$, $\boldsymbol{r}_r = [x_r,\, y_r]^{\mathsf{T}}$, $\tilde{\boldsymbol{w}}_r = \left[\tilde{w}_x,\, \tilde{w}_y,\, \tilde{w}_{\delta t_r},\, \tilde{w}_{\dot{\delta t}_r}\right]^{\mathsf{T}}$,

$$\mathbf{A}_{\mathbf{r}} = \begin{bmatrix} \mathbf{0_{2\times 2}} & \mathbf{I_{2\times 2}} & \mathbf{0_{2\times 2}} \\ \mathbf{0_{2\times 2}} & \mathbf{0_{2\times 2}} & \mathbf{0_{2\times 2}} \\ \mathbf{0_{2\times 2}} & \mathbf{0_{2\times 2}} & \mathbf{A}_{\mathrm{clk}} \end{bmatrix}, \quad \mathbf{D}_{\mathbf{r}} = \begin{bmatrix} \mathbf{0_{2\times 4}} \\ \mathbf{I_{4\times 4}} \end{bmatrix},$$

The receiver's dynamics in (14) is discretized at a sampling period $T \triangleq t_{k+1} - t_k$ to yield the DT-equivalent model

$$\boldsymbol{x}_r\left(t_{k+1}\right) = \mathbf{F}_r\, \boldsymbol{x}_r(t_k) + \boldsymbol{w}_r(t_k), \quad k = 0, 1, 2, \ldots \tag{15}$$

where $\boldsymbol{w}_r$ is a DT zero-mean white noise sequence with covariance $\mathbf{Q}_{\mathbf{r}}$, with

$$\mathbf{F}_{\mathbf{r}} = \begin{bmatrix} \mathbf{I_{2\times 2}} & T\mathbf{I_{2\times 2}} & \mathbf{0_{2\times 2}} \\ \mathbf{0_{2\times 2}} & \mathbf{I_{2\times 2}} & \mathbf{0_{2\times 2}} \\ \mathbf{0_{2\times 2}} & \mathbf{0_{2\times 2}} & \mathbf{F}_{\mathrm{clk}} \end{bmatrix}, \quad \mathbf{F}_{\mathrm{clk}} = \begin{bmatrix} 1 & T \\ 0 & 1 \end{bmatrix}$$

$$\mathbf{Q_r} = \text{diag}\left[\mathbf{Q}_{\text{pv}},\, \mathbf{Q}_{\text{clk,r}}\right],\ \mathbf{Q}_{\text{clk,r}} = \begin{bmatrix} S_{\delta t_r} T + S_{\dot{\delta t}_r} \frac{T^3}{3} & S_{\dot{\delta t}_r} \frac{T^2}{2} \\ S_{\dot{\delta t}_r} \frac{T^2}{2} & S_{\dot{\delta t}_r} T \end{bmatrix}$$

$$\mathbf{Q}_{\text{pv}} = \begin{bmatrix} \tilde{q}_x \frac{T^3}{3} & 0 & \tilde{q}_x \frac{T^2}{2} & 0 \\ 0 & \tilde{q}_y \frac{T^3}{3} & 0 & \tilde{q}_y \frac{T^2}{2} \\ \tilde{q}_x \frac{T^2}{2} & 0 & \tilde{q}_x T & 0 \\ 0 & \tilde{q}_y \frac{T^2}{2} & 0 & \tilde{q}_y T \end{bmatrix}.$$

For simplicity, the SOP will be assumed to emanate from a spatially-stationary terrestrial transmitter and its state will consist of its planar position and clock error states. Hence, the SOP's dynamics can be described by the LTI state-space model

$$\dot{\boldsymbol{x}}_s(t) = \mathbf{A}_s\, \boldsymbol{x}_s(t) + \mathbf{D}_s \tilde{\boldsymbol{w}}_s(t), \tag{16}$$

where $\boldsymbol{x}_s = \left[\boldsymbol{r}_s^{\mathsf{T}},\, \delta t_s,\, \dot{\delta t}_s\right]^{\mathsf{T}}$, $\boldsymbol{r}_s = [x_s,\, y_s]^{\mathsf{T}}$, $\boldsymbol{w}_s = \left[\tilde{w}_{\delta t_s},\, \tilde{w}_{\dot{\delta t}_s}\right]^{\mathsf{T}}$

$$\mathbf{A_s} = \begin{bmatrix} \mathbf{0_{2\times 2}} & \mathbf{0_{2\times 2}} \\ \mathbf{0_{2\times 2}} & \mathbf{A}_{\text{clk}} \end{bmatrix}, \quad \mathbf{D_s} = \begin{bmatrix} \mathbf{0_{2\times 2}} \\ \mathbf{I_{2\times 2}} \end{bmatrix},$$

Discretizing the SOP's dynamics (16) at a sampling interval T yields the DT-equivalent model

$$\boldsymbol{x}_s\left(t_{k+1}\right) = \mathbf{F}_s\, \boldsymbol{x}_s(t_k) + \boldsymbol{w}_s(t_k), \tag{17}$$

where $\boldsymbol{w}_s$ is a DT zero-mean white noise sequence with covariance $\mathbf{Q_s}$, and

$$\mathbf{F_s} = \text{diag}\left[\mathbf{I_{2\times 2}},\, \mathbf{F}_{\text{clk}}\right], \quad \mathbf{Q_s} = \text{diag}\left[\mathbf{0_{2\times 2}},\, \mathbf{Q}_{\text{clk,s}}\right],$$

where $\mathbf{Q}_{\text{clk,s}}$ is identical to $\mathbf{Q}_{\text{clk,r}}$, except that the spectra $S_{\delta t_r}$ and $S_{\dot{\delta t}_r}$ are now replaced with SOP-specific spectra, $S_{\delta t_s}$ and $S_{\dot{\delta t}_s}$.

Defining the augmented state as $\boldsymbol{x} \triangleq \left[\boldsymbol{x}_r^{\mathsf{T}},\, \boldsymbol{x}_s^{\mathsf{T}}\right]^{\mathsf{T}}$ and the augmented process noise vector as $\boldsymbol{w} \triangleq \left[\boldsymbol{w}_r^{\mathsf{T}},\, \boldsymbol{w}_s^{\mathsf{T}}\right]^{\mathsf{T}}$ yields the system dynamics

$$\boldsymbol{x}\left(t_{k+1}\right) = \mathbf{F}\, \boldsymbol{x}\left(t_k\right) + \boldsymbol{w}(t_k), \tag{18}$$

where $\mathbf{F} = \text{diag}\left[\mathbf{F_r},\, \mathbf{F_s}\right]$, and $\boldsymbol{w}$ is a zero-mean white noise sequence with covariance $\mathbf{Q} = \text{diag}\left[\mathbf{Q_r}, \mathbf{Q_s}\right]$. While the model defined in (18) considered only one receiver and one SOP, the model can be readily extended to multiple receivers and SOPs by augmenting their corresponding states and dynamics.

B. Observation Model

To properly model the pseudorange observations, one must consider three different time systems. The first is true time, denoted by the variable t, which can be considered equivalent to GPS system time. The second time system is that of the receiver's clock and is denoted t_r. The third time system is that of the SOP's clock and is denoted t_s. The three time systems are related to each other according to

$$t = t_r - \delta t_r(t) \tag{19}$$

$$t = t_s - \delta t_s(t), \tag{20}$$

where $\delta t_r(t)$ and $\delta t_s(t)$ represent the amount by which the receiver and SOP clocks are different from true time, respectively.

The pseudorange observation made by the receiver on a particular SOP is made in the receiver time and is modeled according to

$$\begin{aligned} \rho(t_r) = {} & \\ & \left\|\boldsymbol{r}_r\left[t_r - \delta t_r(t_r)\right] - \boldsymbol{r}_s\left[t_r - \delta t_r(t_r) - \delta t_{\text{TOF}}\right]\right\|_2 + \\ & c\,.\left\{\delta t_r(t_r) - \delta t_s\left[t_r - \delta t_r(t_r) - \delta t_{\text{TOF}}\right]\right\} + \tilde{v}_\rho(t_r), \end{aligned} \tag{21}$$

where c is the speed of light, δt_{TOF} is the time-of-flight of the signal from the SOP to the receiver, and $\tilde{v}_\rho$ is the error in the pseudorange measurement due to modeling and measurement errors. The error $\tilde{v}_\rho$ is modeled as a zero-mean white Gaussian noise process with power spectral density $\tilde{r}$ [19]. In (21), the clock offsets δt_r and δt_s were assumed to be small and slowly changing, in which case $\delta t_r(t) = \delta t_r\left[t_r - \delta t_r(t)\right] \approx \delta t_r(t_r)$. The first term in (21) is the true range between the receiver's position at time of reception and the SOP's position at time-of-transmission of the signal, while the second term arises due to the offsets from true time in the receiver and SOP clocks.

The observation model in the form of (21) is inappropriate for our observability analysis as it suffers from two shortcomings: (i) it is in a time system that is different from the one considered in deriving the system dynamics, and (ii) the observation model is a nonlinear function of the delayed system states. The first shortcoming can be dealt with by converting the observation model to true time. The second problem is commonly referred to as the output delay problem, in which the observations (outputs) are a delayed version, deterministic or otherwise, of the system state. A common approach to deal with this problem entails discretizaion and state augmentation [20]. For simplicity, and in order not to introduce additional states in our model, proper approximations will be invoked to deal with the second shortcoming.

To this end, the pseudorange observation model in (21) is converted to true time by invoking the relationship (19) to get an observation model for $\rho[t+\delta t_r(t)]$. The resulting observation model is delayed by $\delta t_r(t)$ to get an observation model for $\rho(t)$. Assuming the receiver's position to be approximately stationary within a time interval of $\delta t_r(t)$, i.e. $\boldsymbol{r}_r\left[t - \delta t_r(t)\right] \approx \boldsymbol{r}_r(t)$, and using the fact that the SOP's position is stationary, i.e. $\boldsymbol{r}_s\left[t - \delta t_r(t) - \delta t_{\text{TOF}}\right] = \boldsymbol{r}_s(t)$,

yields

$$\rho(t) \approx \|\boldsymbol{r}_r(t) - \boldsymbol{r}_s(t)\|_2 + c\,.\,\{\delta t_r(t) - \delta t_s\,[t - \delta t_r(t) - \delta t_{\text{TOF}}]\} + \tilde{v}_\rho(t). \quad (22)$$

Next, it is argued that $\delta t_s\,[t - \delta t_r(t) - \delta t_{\text{TOF}}] \approx \delta t_s\,(t)$. The validity of this argument depends on the size of δt_r and of δt_{TOF} and on the rate of change of δt_s. For ground-based SOP transmitters up to 1 km away, the time-of-flight δt_{TOF} is less than $3.34\,\mu$s. Likewise, the offset δt_r can be assumed to be on the order of microseconds. It is reasonable to assume the SOP clock bias δt_s to have an approximately constant value over microsecond time intervals. Therefore, the pseudorange observation model can be further simplified and expressed as a nonlinear function of the state as

$$\begin{aligned} z(t) = \rho(t) &\triangleq h\,[\boldsymbol{x}(t)] + \tilde{v}_\rho(t) \\ &\approx \|\boldsymbol{r}_r(t) - \boldsymbol{r}_s(t)\|_2 + c\,\cdot\,[\delta t_r(t) - \delta t_s(t)] + \tilde{v}_\rho(t). \end{aligned} \quad (23)$$

Discretizing the observation equation (23) at a sampling interval T yields the DT-equivalent observation model

$$\begin{aligned} z(t_k) &= y(t_k) + v_\rho(t_k) \\ &= \|\boldsymbol{r}_r(t_k) - \boldsymbol{r}_s(t_k)\|_2 + c\,\cdot\,[\delta t_r(t_k) - \delta t_s(t_k)] + v_\rho(t_k), \end{aligned} \quad (24)$$

where v_ρ is a DT zero-mean, white Gaussian process with covariance $r = \tilde{r}/T$.

IV. OBSERVABILITY ANALYSIS OF COPNAV ENVIRONMENTS

A. Observability Analysis Objective

This section establishes the various conditions under which a COpNav environment is observable. The objective of this analysis is twofold: (i) determine whether the environment is observable, and (ii) if the environment is not completely observable, determine the observable states, if any. To this end, the nonlinear observability matrix defined in (9) and the l-step observability matrix defined in (3) will be utilized.

B. Receiver Trajectory Singularity

In the upcoming analysis, it is assumed that the receiver is not stationary and that its trajectory is not collinear with the vectors connecting the receiver and any of the SOPs. It is assumed that $\nexists\ \alpha \in \mathbb{R}$ such that $\dot{x}_r(t_{k+1}) = \alpha\,[x_r(t_k) - x_s(t_k)]$ and $\dot{y}_r(t_{k+1}) = \alpha\,[y_r(t_k) - y_s(t_k)]$. This ensures that the bearing angle between the receiver and the SOPs is never constant along the receiver trajectory. This assumption ensures that the observability matrix will not lose rank due to the receiver's motion path.

To illustrate why this case must be excluded, consider a simplified scenario in which the receiver and SOP clocks are ideal such that the observations are given by $y(t_k) = \|\boldsymbol{r}_r(t_k) - \boldsymbol{r}_s(t_k)\|_2$. In this case, the state vector is given by $\boldsymbol{x} = \left[\boldsymbol{r}_r^\mathsf{T},\, \dot{\boldsymbol{r}}_r^\mathsf{T}, \boldsymbol{r}_s^\mathsf{T}\right]^\mathsf{T}$ and the corresponding observability matrix is given by

$$\boldsymbol{\mathcal{O}}(t_0, t_l) = \begin{bmatrix} \mathbf{h}_{a,r,s}^\mathsf{T}(t_0) & \mathbf{0}_{2\times 1} & -\mathbf{h}_{a,r,s}^\mathsf{T}(t_0) \\ \mathbf{h}_{a,r,s}^\mathsf{T}(t_1) & T\mathbf{h}_{a,r,s}^\mathsf{T}(t_1) & -\mathbf{h}_{a,r,s}^\mathsf{T}(t_1) \\ \vdots & \vdots & \vdots \\ \mathbf{h}_{a,r,s}^\mathsf{T}(t_{l-1}) & T(l-1)\mathbf{h}_{a,r,s}^\mathsf{T}(t_{l-1}) & -\mathbf{h}_{a,r,s}^\mathsf{T}(t_{l-1}) \end{bmatrix},$$

where $\mathbf{h}_{a,r,s}^\mathsf{T}(t_k) \triangleq \left[\frac{x_r(t_k)-x_s(t_k)}{\|\boldsymbol{r}_r(t_k)-\boldsymbol{r}_s(t_k)\|_2}, \frac{y_r(t_k)-y_s(t_k)}{\|\boldsymbol{r}_r(t_k)-\boldsymbol{r}_s(t_k)\|_2}\right]$. An alternative expression for $\mathbf{h}_{a,r,s}^\mathsf{T}(t_k)$ is given by $\mathbf{h}_{a,r,s}^\mathsf{T}(t_k) = [\cos\theta_{r,s}(t_k),\, \sin\theta_{r,s}(t_k)\,]$, where $\theta_{r,s}(t_k)$ is the angle between the x-axis and the range vector connecting the receiver and the SOP at time instant t_k. In this representation, it becomes obvious that $\boldsymbol{\mathcal{O}}_L(t_0, t_l)$ has a rank of 3 except when the receiver's motion path is collinear with the SOP, in which case it has a rank of 2, since in this case $\theta_{r,s}(t_0) = \theta_{r,s}(t_1) = \ldots = \theta_{r,s}(t_{l-1})$.

C. Scenarios Overview

The various scenarios considered in the observability analysis are outlined Table I. The first scenario corresponds to a single receiver and a single SOP whose initial states are unknown (no *a priori* knowledge about any of the states is available). Subsequent scenarios consider cases of partial or full knowledge of initial states. In Table I, fully-known means that all the initial states are known. Thus, a fully-known receiver is one with known $\boldsymbol{x}_r(t_0)$, whereas a fully-known SOP is one with known $\boldsymbol{x}_s(t_0)$. On the other hand, partially-known means that only the initial position states are known. Thus, a partially-known receiver is one with known $\boldsymbol{r}_r(t_0)$, whereas a partially-known SOP is one with known $\boldsymbol{r}_s(t_0)$.

TABLE I
COPNAV OBSERVABILITY ANALYSIS SCENARIOS CONSIDERED

Case	Receiver(s)	SOP(s)
1	1 Unknown	1 Unknown
2	1 Unknown	m Partially-known
3	1 Unknown	1 Fully-known
4	1 Unknown	1 Fully-known & 1 Partially-known
5	n Partially-known	1 Unknown
6	n Partially-known	m Partially-known
7	1 Partially-known	1 Fully-known
8	1 Fully-known	1 Unknown

D. Observability Analysis Results

The nonlinear and linear observability tests discussed in Section II were applied to the scenarios outlined in Table I. The conclusions achieved through both tests coincided and are summarized in Table II. It is worth noting that the observability results constitute the minimal set of observability requirements in the sense that knowing the results for these scenarios, one can predict the observability of an arbitrary scenario with n receivers and m SOPs and any type of prior knowledge (none, partial, or full) for the receivers and SOPs.

TABLE II
COPNAV OBSERVABILITY ANALYSIS RESULTS

Case	Observable?	Observable States
1	no	none
2	no	$m = 1$: none $m \geq 2$: x_r, y_r, $\dot{x}_r$, $\dot{y}_r$
3	no	δt_r, $\dot{\delta t}_r$
4	yes	all
5	no	$\dot{x}_{r_i}$, $\dot{y}_{r_i}$, x_s, y_s, $i = 1, \ldots, n$
6	no	$\dot{x}_{r_i}$, $\dot{y}_{r_i}$, $i = 1, \ldots, n$
7	yes	all
8	yes	all

V. ESTIMABILITY ANALYSIS OF COPNAV ENVIRONMENTS

This section presents the estimability analysis results that were achieved by simulating the three observable cases in Table I: cases 4, 7, and 8. For purposes of numerical stability, the clock error states were defined to be $c\delta t$ and $c\dot{\delta t}$. All simulations assumed the receiver's process noise spectral density to be $\tilde{q}_x = \tilde{q}_y = 0.001\,\mathrm{m}^2/\mathrm{s}^4$, while the sampling period was set to $T = 1$ ms. The receiver's clock was assumed to be a temperature-compensated crystal oscillator (TCXO) with $h_0 = 2 \times 10^{-19}$ and $h_{-2} = 2 \times 10^{-20}$, while the SOPs' clocks were assumed to be oven-controlled crystal oscillators (OCXOs) with $h_0 = 8 \times 10^{-20}$ and $h_{-2} = 4 \times 10^{-23}$.

A simulator was developed to generate the "truth" data for each COpNav environment studied. Noisy pseudorange observations were processed by an Extended Kalman Filter (EKF) to estimate the states of interest. The observability and estimability were quantified in terms of the estimation error $\tilde{\boldsymbol{x}} \triangleq \boldsymbol{x} - \hat{\boldsymbol{x}}$ and the corresponding estimation error covariance $\mathbf{P} \triangleq \mathbb{E}\left[\tilde{\boldsymbol{x}}\,\tilde{\boldsymbol{x}}^{\mathsf{T}}\right]$, where $\hat{\boldsymbol{x}}$ is the EKF state estimate.

In the following simulations, the system true initial state $\boldsymbol{x}(t_0)$ was fixed, while the EKF initial state estimate $\hat{\boldsymbol{x}}(t_0)$ was generated according to $\hat{\boldsymbol{x}}(t_0) \sim \mathcal{N}\left[\boldsymbol{x}(t_0), \mathbf{P}(t_0|t_{-1})\right]$, where $\mathbf{P}(t_0|t_{-1})$ is the EKF initial estimation error covariance. All the simulations assumed a receiver whose initial state is $\boldsymbol{x}_r(t_0) = [0,\, 0,\, 0,\, 250,\, 10,\, 10]^{\mathsf{T}}$ and SOPs with initial states $\boldsymbol{x}_{s_1}(t_0) = [50,\, 50,\, 10,\, 10]^{\mathsf{T}}$ and $\boldsymbol{x}_{s_2}(t_0) = [-50,\, 50,\, 10,\, 10]^{\mathsf{T}}$.

The simulations for Case 4 considered an environment with an unknown receiver and two SOPs, one fully-known and one partially-known. The observation noise spectral density was set to $r = 25\,\mathrm{m}^2$. The initial estimation error covariance matrices of the receiver and the second SOP were chosen to be $\mathbf{P}_r(t_0|t_{-1}) = \mathrm{diag}\left[100, 100, 100, 100, 3 \times 10^4, 300\right]$ and $\mathbf{P}_{s_2}(t_0|t_{-1}) = \mathrm{diag}\left[3 \times 10^4, 300\right]$, respectively.

The simulations for Case 7 considered an environment with a partially-known receiver and two SOPs, one fully-known and one unknown. The observation noise spectral density was set to $r = 100\,\mathrm{m}^2$. The initial estimation error covariance matrices of the receiver and the second SOP were chosen to be $\mathbf{P}_r(t_0|t_{-1}) = \mathrm{diag}\left[100, 100, 3 \times 10^4, 300\right]$ and $\mathbf{P}_{s_2}(t_0|t_{-1}) = \mathrm{diag}\left[100, 100, 3 \times 10^4, 300\right]$, respectively.

The simulations for Case 8 considered an environment with a fully-known receiver and one unknown SOP. The observation noise spectral density was set to $r = 100\,\mathrm{m}^2$. The initial estimation error covariance matrix of the SOP was chosen to be $\mathbf{P}_{s_1}(t_0|t_{-1}) = \mathrm{diag}\left[100, 100, 3 \times 10^4, 300\right]$, respectively.

Figures 1, 2, and 3 show the estimation error trajectories $\tilde{x}_i(t_k|t_k)$ for a single-run EKF along with the $\pm 2\sigma_i(t_k|t_k)$ estimation error variance bounds for cases 4, 7, and 8, respectively. Note that the estimation error covariance converge and that the estimation errors remain bounded, as would be expected for an observable system.

The eigenvalues associated with the normalized estimation error covariance (13) in ascending order at the end of the simulation are given in Table III. It is noted that in all three cases there is a wide dispersion between the smallest and largest eigenvalues, indicating the existence of modes with exceptionally good and exceptionally poor observability. To determine the directions associated with the modes with good and poor observability, the eigenvectors corresponding to the smallest and largest eigenvalues are calculated and plotted in Figures 4, 5, and 6, respectively. From Figure 4 it can be concluded that the linear combination of the fifth and seventh states, corresponding to δt_r and δt_s, can be estimated exceptionally well with respect to the rest of the states, whereas a linear combination of the second, fourth, and sixth states, corresponding to y_r, $\dot{y}_r$, and y_s, are poorly observable. From Figure 5 it can be concluded that the first and second states, corresponding to $\dot{x}_r$ and $\dot{y}_r$, can be estimated exceptionally well with respect to the rest of the states, whereas a linear combi-

nation of the fifth, sixth, and eighth states, corresponding to x_{s_2}, y_{s_2}, and $\delta\dot{t}_{s_2}$, are poorly observable. From Figure 6 it can be concluded that the third state, corresponding to δt_s, can be estimated exceptionally well with respect to the rest of the states, whereas a linear combination of the first, second, and fourth states, corresponding to x_s, y_s, and $\dot{\delta}t_s$, are poorly observable.

TABLE III
EIGENVALUES OF NORMALIZED ESTIMATION ERROR COVARIANCE MATRIX FOR COPNAV OBSERVABLE SCENARIOS

Case	Eigenvalues
4	1.07×10^{-5}, 5.56×10^{-5}, 5.71×10^{-3}, 1.53×10^{-2}, 4.00×10^{-2}, 6.95×10^{-1}, 2.27, 4.97
7	1.19×10^{-7}, 1.19×10^{-7}, 5.78×10^{-5}, 3.60×10^{-4}, 4.82×10^{-2}, 2.56×10^{-1}, 1.14, 6.56
8	7.27×10^{-5}, 3.67×10^{-2}, 5.08×10^{-1}, 3.45

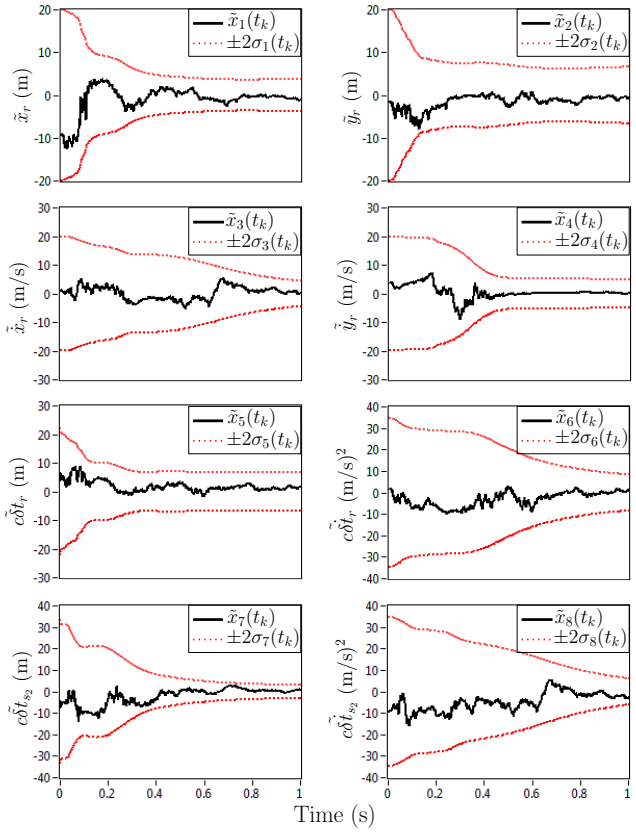

Fig. 1. Estimation error trajectories and $\pm 2\sigma$-bounds for case 4 in Table I

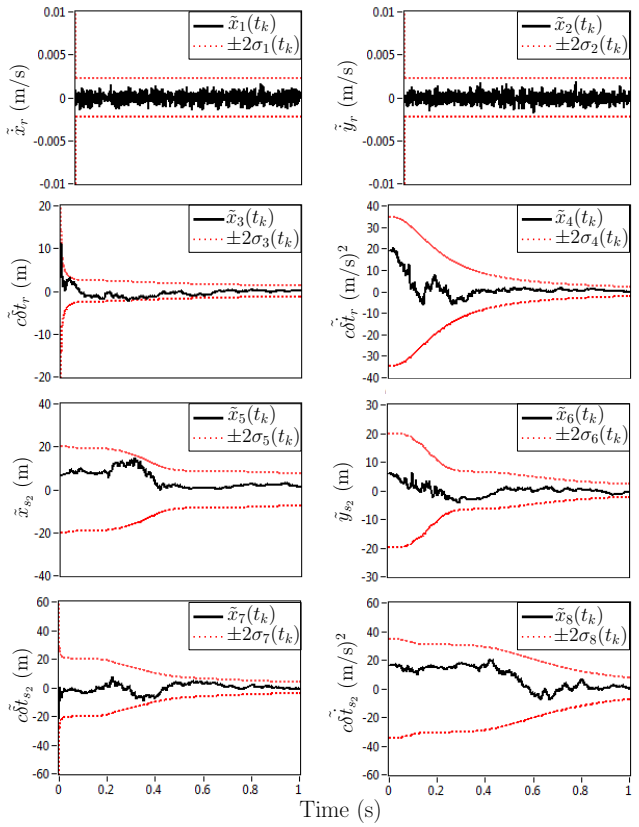

Fig. 2. Estimation error trajectories and $\pm 2\sigma$-bounds for case 7 in Table I

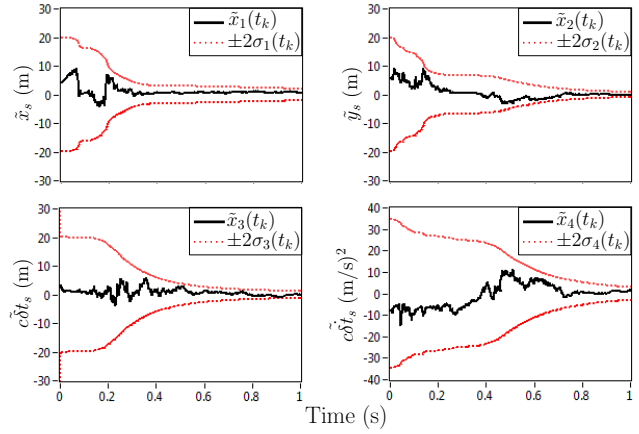

Fig. 3. Estimation error trajectories and $\pm 2\sigma$-bounds for case 8 in Table I

VI. CONCLUSIONS

This paper studied the observability and estimability of COpNav environments. It was concluded that a planar COpNav environment consisting of n receivers with velocity random walk dynamics making pseudorange measurements on m stationary SOPs is fully-observable if and only if the initial state(s) of: at least one receiver is fully-known, or at least one receiver is partially-known and at least one

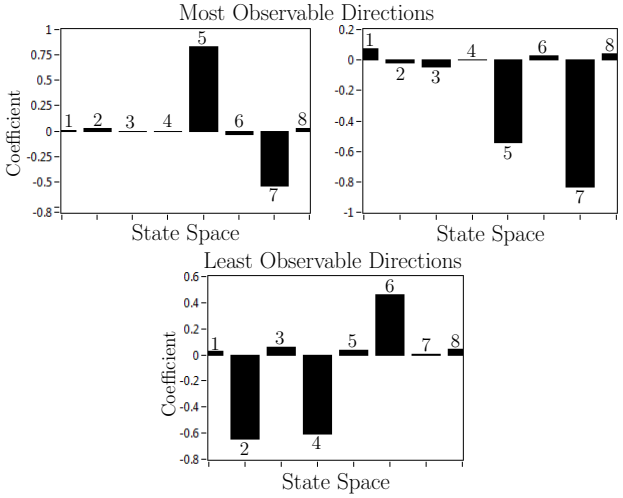

Fig. 4. Eigenvector along the most and least observable directions in the state space for case 4 in Table I

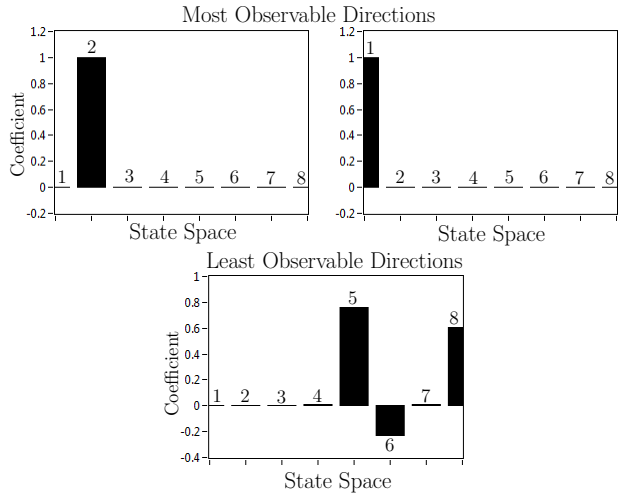

Fig. 5. Eigenvector along the most and least observable directions in the state space for case 7 in Table I

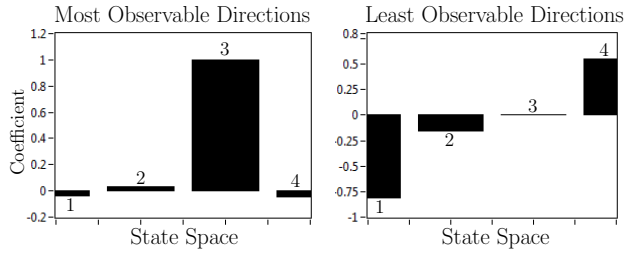

Fig. 6. Eigenvector along the most and least observable directions in the state space for case 8 in Table I

SOP is fully-known, or at least one SOP is fully-known and at least one SOP is partially-known. For the observable scenarios, the estimability of the various states in the environment was analyzed, with particular attention paid to the directions with exceptionally good and poor observability.

References

[1] K. Pesyna, Z. Kassas, J. Bhatti, and T. Humphreys, "Tightly-coupled opportunistic navigation for deep urban and indoor positioning," in *Proceedings of the International Technical Meeting of The Satellite Division of the Institute of Navigation (ION GNSS)*, vol. 1, September 2011, pp. 3605–3617.

[2] K. Pesyna, Z. Kassas, and T. Humphreys, "Constructing a continuous phase time history from TDMA signals for opportunistic navigation," in *IEEE/ION Position Location and Navigation Symposium (PLANS)*, April 2012, pp. 1209–1220.

[3] J. J. Spilker, Jr, *Global Positioning System: Theory and Applications*. Washington, D.C.: American Institute of Aeronautics and Astronautics, 1996, ch. 2: Overview of GPS Operation and Design, pp. 57–119.

[4] H. Durrant-Whyte and T. Bailey, "Simultaneous localization and mapping: part I," *IEEE Robotics & Automation Magazine*, vol. 13, no. 2, pp. 99–110, June 2006.

[5] J. Andrade-Cetto and A. Sanfeliu, "The effects of partial observability when building fully correlated maps," *IEEE Transactions on Robotics*, vol. 21, no. 4, pp. 771–777, August 2005.

[6] T. Vida-Calleja, M. Bryson, S. Sukkarieh, A. Sanfeliu, and J. Andrade-Cetto, "On the observability of bearing-only SLAM," in *Proceedings of IEEE Internartional Conference on Robotics and Automation*, vol. 1, April 2007, pp. 4114–4118.

[7] K. Lee, W. Wijesoma, and I. Javier, "On the observability and observability analysis of SLAM," in *Proceedings of IEEE Internartional Conference on Intelligent Robots and Systems*, vol. 1, October 2006, pp. 3569–3574.

[8] Z. Wang and G. Dissanayake, "Observability analysis of SLAM using Fisher information matrix," in *Proceedings of IEEE International Conference on Control, Automation, Robotics, and Vision*, vol. 1, December 2008, pp. 1242–1247.

[9] L. Perera, A. Melkumyan, and E. Nettleton, "On the linear and nonlinear observability analysis of the SLAM problem," in *Proceedings of IEEE Internartional Conference on Mechatronics*, vol. 1, April 2009, pp. 1–6.

[10] D. Goshen-Meskin and I. Bar-Itzhack, "Observability analysis of piece-wise constant systems–part I: Theory," *IEEE Transactions on Aerospace and Electronic Systems*, vol. 28, no. 4, pp. 1056–1067, October 1992.

[11] Z. Kassas and T. Humphreys, "Observability analysis of opportunistic navigation with pseudorange measurements," in *Proceedings of AIAA Guidance, Navigation, and Control Conference*, vol. 1, August 2012, pp. 4760–4775.

[12] R. Hermann and A. Krener, "Nonlinear controllability and observability," *IEEE Transactions on Automatic Control*, vol. 22, no. 5, pp. 728–740, October 1977.

[13] M. Anguelova, "Observability and identifiability of nonlinear systems with applications in biology," Ph.D. dissertation, Chalmers University Of Technology and Göteborg University, Sweden, 2007.

[14] J. Casti, "Recent developments and future perspectives in nonlinear system theory," *SIAM Review*, vol. 24, no. 3, pp. 301–331, July 1982.

[15] W. Respondek, "Geometry of static and dynamic feedback," in *Lecture Notes at the Summer School on Mathematical Control Theory*, Trieste, Italy, September 2001.

[16] W. Rugh, *Linear System Theory*, 2nd ed. Upper Saddle River, NJ: Prentice Hall, 1996.

[17] Y. Bar-Shalom, X. Li, and T. Kirubarajan, *Estimation with Applications to Tracking and Navigation*, 1st ed. New York, NY: John Wiley & Sons, 2002.

[18] F. Ham and R. Brown, "Observability, eigenvalues, and Kalman filtering," *IEEE Transactions on Aerospace and Electronic Systems*, vol. 19, no. 2, pp. 269–273, March 1983.

[19] M. Psiaki and S. Mohiuddin, "Modeling, analysis, and simulation of GPS carrier phase for spacecraft relative navigation," *Journal of Guidance, Control, and Dynamics*, vol. 30, no. 6, pp. 1628–1639, November-December 2007.

[20] Z. Kassas, "Discretisation of continuous-time dynamic multi-input multi-output systems with non-uniform delays," *IET Proceedings on Control Theory & Applications*, vol. 5, no. 14, pp. 1637–1647, September 2011.